Progress in Energy and Environment

Original Article

Enhancing solar hybrid system efficiency in Libya through PSO & flower pollination optimization

OPEN ACCESS

Ahmed Moh A Al Smin[1] (ID), Alkbir Munir Faraj Almabrouk[2,*] (ID), Sairul Izwan Bin Safie[2] (ID), Mohd Al Fatihhi Bin Mohd Szali Januddi[2] (ID), Mohd Fahmi Bin Hussin[1] (ID), Abdulgader Alsharif[3] (ID)

[1] Electrical Department, University Kuala Lumpur British Malaysian Institute (UniKL BMI), Batu 8, Jln Sg. Pusu, 53100, Gombak, Malaysia
[2] Malaysian Institute of Industrial Technology, University Kuala Lumpur (UniKL MITEC), Persiaran Sinaran Ilmu, Bandar Seri Alam, 81750, Johor, Malaysia
[3] Department of Electrical and Electronic Engineering, Faculty of Technical Sciences, Sabha, Libya
* Correspondence email: munir@unikl.edu.my

Abstract

The integration and optimization of Concentrated Solar Power-Photovoltaic (CSP-PV) hybrid systems have become a focal point in the field of solar energy research and development. The fusion of the strengths from both forms of power generation in the CSP-PV hybrid system offers the potential to deliver affordable and manageable solar energy solutions. However, the key parameters of the CSP plant can vary in different situations. Taking these variations into account is crucial for optimizing the overall performance of the CSP-PV hybrid system and ensuring its adaptability to different scenarios. Therefore, there is a need for a method that can optimize all the main parameters of the CSP and the hybrid system at the same time. The maximum acquired energy from the CSP is 7 kWh with meeting the objective of Levelized Cost of Energy (LCOE). In this paper utilized the Flower Pollination Algorithm (FPA). method to globally optimize the CSP-PV Hybrid System. The experimental results prove the effectiveness of this method.

1 Introduction

Solar energy is an abundant and renewable energy source [1]. The installed capacity of solar energy has been growing sharply in recent years [2]. In the commercial application of solar energy, two basic categories of technology are prominently utilized, namely, PV technology and CSP technology. PV technology has experienced substantial commercialization and cost reduction. However, it is subject to major influence from Global Horizontal Irradiance (GHI). On the other hand, the thermal storage component of CSP technology allows for greater operational flexibility depending on the level of Direct Normal Irradiance (DNI). However, because of its small-scale manufacture, this technology is more expensive [3]. Therefore, the hybridization of a PV system and a CSP system is regarded as an important solution to the aforementioned dilemma [4]. Some works optimize the proportional relationship just by considering the installation scale of the two kinds of technologies. However, as a complex system, the parameters of a single CSP system also need to change based on different application scenarios. Moreover, previous studies have indicated that the Levelized Cost of Energy (LCOE) for CSP systems is significantly influenced by crucial system characteristics like as the solar multiple, the duration of storage hours at maximum capacity, turbine output, and other related aspects. Therefore, a method with the ability to optimize all

these parameters in different levels of the CSP-PV hybrid system is urgently needed. Tripoli, Libya (32°52 N, 13°11 E) is selected as the area of study, and weather data are from the Libyan Centre for Solar Energy Research and Studies. The best tilt angle for solar panels is 35° in Tripoli [5]. Simulation of a hybrid PV-CSP system was ccarried out J.A. Aguilar-Jimenez et al. [1] with thermal energy storage applied to isolated microgrids and analyzed the techno-economic feasibility of this system. The study demonstrates that a hybrid PV-CSP system with thermal energy storage can be economically viable in isolated microgrids with a high share of renewable sources. The study found that such a system can achieve high renewable energy integration rates and improve the energy independence of isolated microgrids [1]. Provided Rongrong Zhai et al [6] with the modeling and simulation of the CSP and PV systems, optimization of the power generation system, and techno-economic analysis of the proposed hybrid power plant [2]. The authors compared different optimization methods and showed that the proposed method can achieve an optimal design with high efficiency and lower cost. The Design of the hybrid power plant integrated a tightly coordinated management strategy to overcome some of the inherent weaknesses of renewable energy resources. The authors also suggested that this optimal design method can be used in the preliminary design of other power stations [6]. In terms of numerical results, the study provides the annual power generation of the PV system (309036 MW) and CSP system (66659 MW). It also details the annual utilization hours of both systems, which are 3201 h and 2222 h, respectively. However, it does not provide detailed numerical data on the comparative analysis of different methods. The structure and energy flow of the autonomous microgrid is presented in Fig. 1. The solid lines (Power line) represent the flow of electrical power, while the dashed (Communication and control line) and dotted (Communication line) lines represent data and control signals that the EMS uses to control the system.
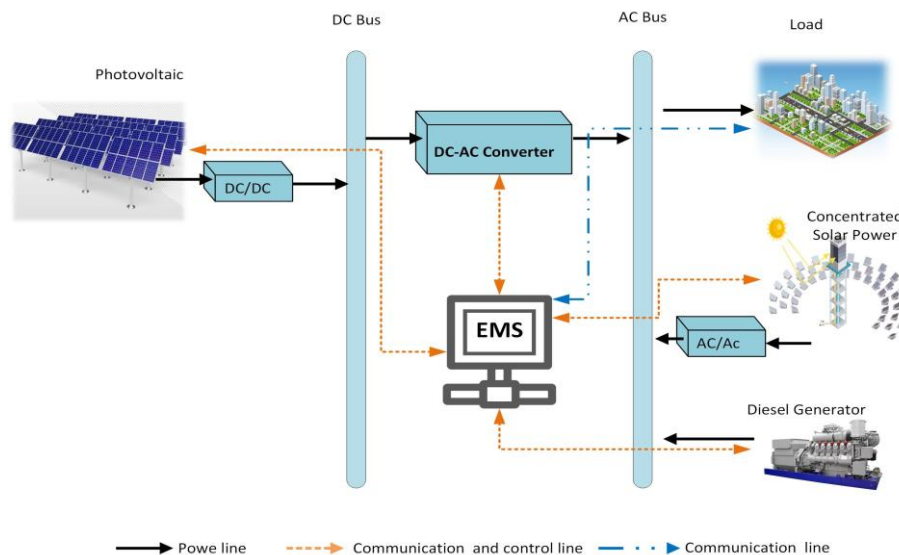

Fig. 1 Microgrid Hybrid PV-CSP.

In this paper, we propose a novel method based on the FPA to address this challenge. Each pollen represents a design scheme for the hybrid system, and as the pollen, we can achieve a group of optimized parameters for the system. The experimental results, based on the real demand curve, demonstrate the effectiveness of this method.

2 Details and modelling of a hybrid CSP-PV system

2.1 Solar energy resources

Solar energy resources refer to the energy harnessed from the sun's rays and converted into usable power for various applications, such as powering homes, businesses, utilities, and more. As solar energy resources have garnered significant attention in recent years [7]. In this study, we focus on both the PV and CSP systems, even though the most important weather factors for each are different. While it depends on the specific requirements and technology of the solar energy system being used. where regarded as DNI is more suitable for CSP systems due to its higher concentration of sunlight. Whereas

GHI is more commonly used in PV systems as it represents the total amount of sunlight available [8]. Fig. 2 shows the photovoltaic power potential in Libya, According to GLOBAL SOLAR ATLAS.
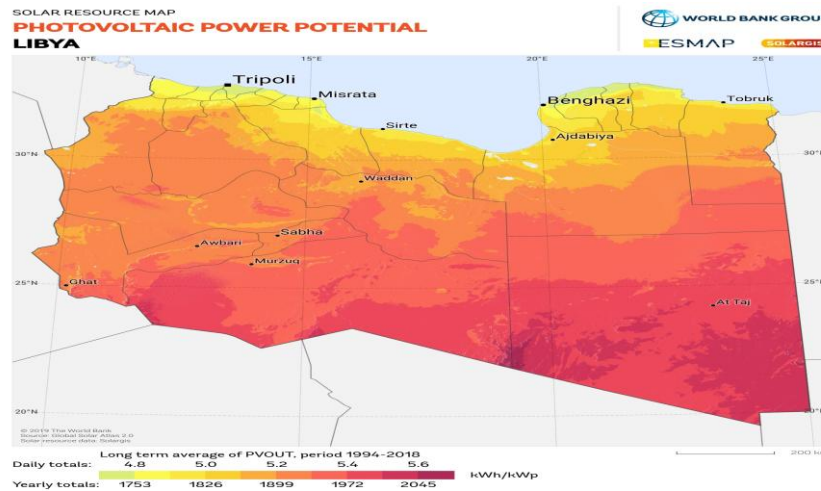

Fig. 2 Solar resource maps of Libya [9].

2.2 Modelling of PV system

PV is the most popular renewable energy source for converting solar energy into electricity. The model equation for the PV system's output power is reported and presented in Equation. The equation is given by [10].

$$PPV(t) = \frac{PPV \text{ rated} \times G(t)}{1000 \cdot [1 + \alpha t(TC - TSTC)]} \tag{1}$$

Herein, $P_{PV}(t)$ represents the generated power output from the PV system in watts, $G_{(t)}$ refers to the hourly solar irradiance data in W/m² [11], with 1000 W/m² denoting the Earth's surface-rated radiation. $P_{PVrated}$ corresponds to the rated power of the PV system in watts. T_{STC} stands for the cell temperature at Standard Test Condition (STC), while α_t represents the temperature coefficient of the panels, set at -3.7×10^{-3} (1/°C) [11]. Furthermore, T_C signifies the cell temperature in degrees.

$$T_c = T_{amb} + G_{(t)} \times \frac{NOCT - 20}{800} \tag{2}$$

T_{amb} signifies the ambient temperature (°C), utilizing time series data. The selected Nominal Operation Cell Temperature (NOCT) for this study is 45°C, based on the specifications of the PV module provided by the manufacturer. The irradiance on the cell surface is set at 800 W/m².

2.3 Modelling of CSP system

The solar tower power generation system is primarily composed of several key components: the heliostat field, the solar tower absorber, a steam turbine, a generator, and a Thermal Energy Storage (TES) system. The heliostat field is comprised of numerous heliostats, each tasked with reflecting sunlight towards the absorber located on the solar tower. The input energy of this subsystem Qsolar can be calculated as follows [12].

2.3.1 Heliostat field model

The heliostat field model can be mathematically expressed as in Eq. (3).

$$Q_{solar} = Af \cdot DNI \tag{3}$$

Here, *DNI* stands for the annual direct normal irradiance of the Project Site, and *Af* denotes the effective area of heliostats. The formula used to calculate the instantaneous energy Q_{rev} incident on the receiver's surface is as follows [13].

$$Q_{rev} = Q_{solar} \cdot \eta_{field} \tag{4}$$

where

$$\eta_{field} = \eta_{hfa} \cdot \eta_{rom} \cdot \eta_{cos} \cdot \eta_{clm} \cdot \eta_{att} \cdot \eta_{sh} \cdot \eta_{bl} \cdot \eta_{spi} \tag{5}$$

Here, η_{hfa} represents the heliostat field availability (Instantaneous), η_{rom} is the specular reflectance of the mirror, η_{cos} represents the cosine efficiency, η_{clm} represents the mirror cleanliness, η_{att} represents the atmospheric attenuation efficiency, η_{sh} represents the shadow efficiency, η_{bl} represents the blocking efficiency, and η_{spi} represents the spill efficiency. The formula for calculating the average annual efficiency is given by the following equation [13].

$$\eta_{field,annual} = \frac{\sum_{day=1}^{365} \int_0^{24} DNI(t)\eta_{field}(t)dt}{\sum_{day=1}^{365} \int_0^{24} DNI(t)dt} \tag{6}$$

2.3.2 Receiver model

The reflected sunlight gets absorbed as thermal energy within the absorber. Energy losses during this process, encompassing optical losses $Q_{loss,opt}$, convective heat losses $Q_{loss,cov}$, and radiation heat losses $Q_{loss,rad}$, are computed in a subsequent manner.

$$Q_{eff} = Q_{receiver} - Q_{loss,opt} - Q_{loss,conv} - Q_{loss,rad} \tag{7}$$

The following method can be used to figure out how much heat the heat transfer fluid (HTF) inside the receiver received in.

$$QHTF = m_{HTF} \cdot (h_{out} - h_{in}) \tag{8}$$

Here, m_{HTF} signifies the mass flow rate of the HTF, while h_{in} and h_{out} represent the specific enthalpy of the HTF at the receiver inlet and outlet, respectively.

2.3.3 TES System

The TES system plays a crucial role within the entire system since it maintains equilibrium and coordinates the distribution of input and output energy at the same time [14]. The following is an equation of the mass balance that may be found in this section [14]:

$$m_{i+1} = m_i + (m_{load} - m_{unload}) \cdot t_{int} \tag{9}$$

Here, the symbols have the following meanings: m_i signifies the mass in the hot tank at the current moment i, while m_{i+1} represents the mass in the hot tank at the subsequent moment $i+1$ (the next moment). Additionally, m_{load} corresponds to the incoming mass of molten salt into the hot tank, and m_{unload} stands for the outgoing mass of molten salt from the hot tank. The symbol t_{int} denotes the computational time unit.

2.3.4 Power block system

The power block system is an essential component of the whole system, and its performance has a direct impact on the plant's system output and revenue. The steam turbine is the most important component of this subsystem, and the primary reason for this is due to the one-of-a-kind qualities that solar thermal power plants possess. There are certain scenarios in which the steam turbine may not work at the circumstances specified in the design. Particularly, fluctuations in temperature and pressure can lead to variations in the mass of the steam turbine. The following formula may be used to compute the conversion relationship for each of the many scenarios [15]:

$$\frac{m_1}{m} = \sqrt{\frac{P_{01}^2 - P_{g1}^2}{P_0^2 - P_g^2}} \sqrt{\frac{T_0}{T_{01}}} \tag{10}$$

where m and m_1 represents the bulk flows of steam under off-design and design conditions, correspondingly. P_0 and P_g are the pressures of the inlet and outlet steams under the design condition,

respectively. P_{01} and P_{g1} are the pressures of the inlet and outlet steams under off-design condition, respectively. T_0 and T_{01} are the inlet steam temperatures under the design and off-design conditions, respectively.

The end output of the plant, which is often talked about in terms of capacity factor, is closely linked to how well this subsystem works. The capacity factor Cf can achieve according to the following formula [16].

$$Cf = \frac{P_{act}}{8760 \cdot P_{nom}} \tag{11}$$

where P_{act} and P_{nom} denote the real and nominal output of the entire system over the course of a full year.

2.3 Diesel Generator Model

In the context of Renewable Energy Sources (RES), power generation depends on the availability of renewable resources. When these resources are unavailable, the energy demand cannot be met. To tackle this issue, a distributed generator (DG) is employed as a supplementary backup within the microgrid. The DG's characteristics are delineated by its fuel consumption (FC), which is defined by the following formula [10]:

$$FC_{(t)} = A_G P_{gen}(t) + B_G P_{gen}(r) \tag{12}$$

In this context, P_{gen} represents the power generated by the DG in kilowatts (kW), while $P_{gen}(r)$ represents the rated power of the DG, also in kilowatts (kW). The coefficients A_G and B_G stand for the fuel consumption coefficients. Common values for these coefficients are $A_G = 0.24$ and $B_G = 0.084$, respectively.

2.4 Inverter Model

An inverter serves to convert DC electricity into AC electricity. The size of the inverter is determined based on accommodating the maximum anticipated AC loads, including potential surges during initial appliance startup. The DC-AC inverter, which connects electrical loads to the grid-independent microgrid, is characterized by its efficiency. Specifically, the inverter efficiency η_{inv} is noted as 95.

$$P_{inv,out}(t) = \left[P_{CSP}(t) + P_{PV}(t) \right] \times \eta_{inv} \tag{13}$$

3. Experimental simulation and performance

The case study is blessed with different climatological conditions in four seasons as high temperature and solar irradiance and the analysis of collected data is a vital task for presenting the comparison and changing during the year. The collected climatology data for the study site have been demonstrated in Fig. (3) for ambient temperature and Direct Normal Irradiance DNI, respectively.

North Africa's dry, hot climate and abundant sunshine give Libya a high GHI. In the southern region, where the Sahara Desert is located, the GHI is relatively higher compared to the northern coastal areas. The area receives intense sunlight throughout the year, and the DNI is often high, especially in the desert regions. This indicates that Libya is an ideal location for solar power projects that require direct sunlight, such as solar thermal power plants, which operate more efficiently under these conditions.

Additionally, the annual obtained comparison output energy from the CSP is shown in Fig. 3 along with the status of other integrated sources. The maximum acquired energy from the CSP is incrementally changing based on the solar irradiance in the considered month. The beginning and the end months of the year as placed in winter are showing high production of energy with more than 7 kWh, while the minimum produced energy with almost 4 kWh. The other sources like battery, thermal and DG are considered with their status during the year in order to meet the demand. Based on the proposed hybrid system with the integration of CSP-PV that is demonstrated in Fig. 3. In Fig. 4 represents the monthly energy production and consumption for a hybrid power system over a year. Each colour corresponds to a different energy source or aspect of energy management. While the output power of the CSP-PV is acquired and plotted in Fig. 5. From the figure, it is clearly seen that the annual output peak is at 15 kWh while the minimum is at 2 kW.
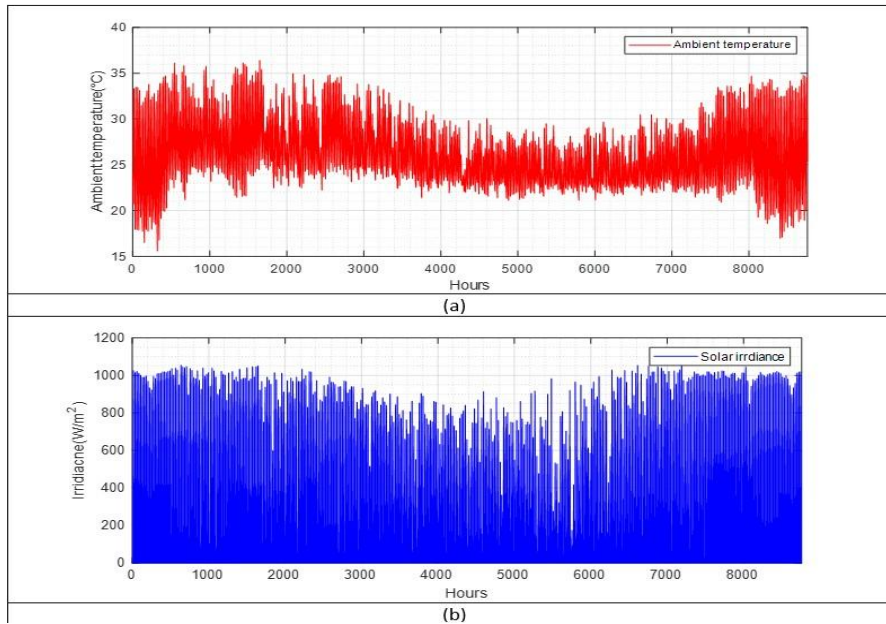
Fig. 3 Geographical data, (a) Ambient temperature and (b) Direct Normal Irradiance DNI.
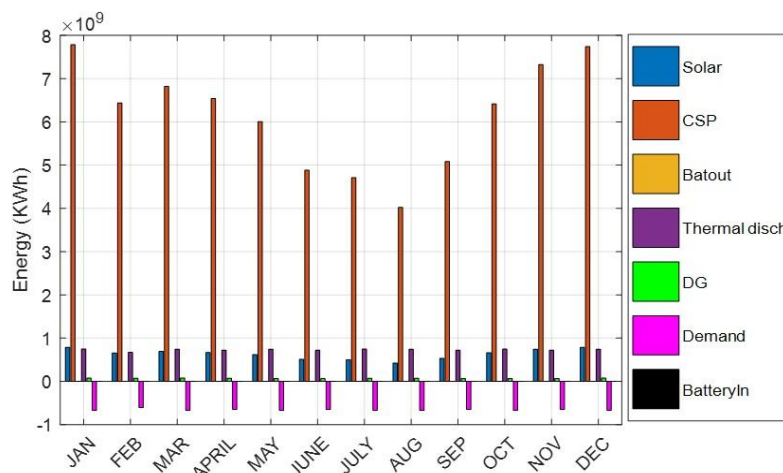

Fig. 4 Comprised output power from the considered sources.

According to the assertions made by Basim Belgasim and other researchers, it is posited that CSP technology holds promise as a significant contributor to sustainable energy generation in the foreseeable future [17]. This is especially applicable to areas characterised by abundant Direct Normal Irradiance (DNI), such as the North African region. Nevertheless, it is important to acknowledge that there exist some technological and economic obstacles that want attention in order to enhance the competitiveness of CSP in comparison to alternative forms of renewable energy [17].

Additionally, the obtained output power from the integrated PV is plotted in Fig. 6 with a peak of 3.7 kW.

Fig. 7 shows a convergence curve that compares the performance of two algorithms: the Flower Pollination Algorithm (FPA) and the Particle Swarm Optimization (PSO). These algorithms are used to find optimal solutions to problems by iterating through possible solutions. The obtained results demonstrate that the FPA outperforms the PSO, as depicted in the figure above, by reducing energy consumption within the hybrid system. This efficiency contributes to an economically advantageous operation of various system components in conjunction with the Energy Management System (EMS).
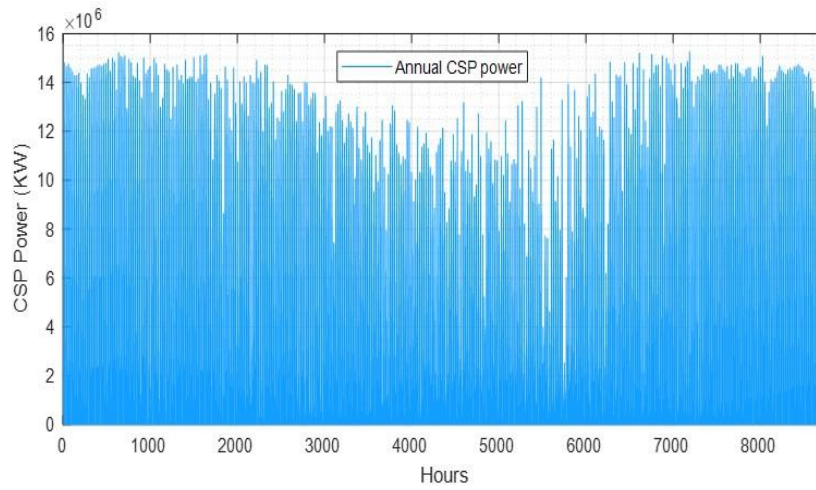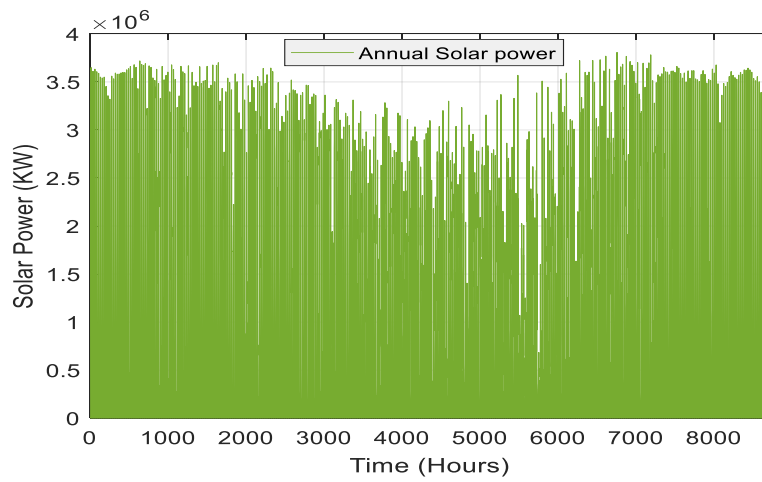
Fig. 5 the output power of CSP.
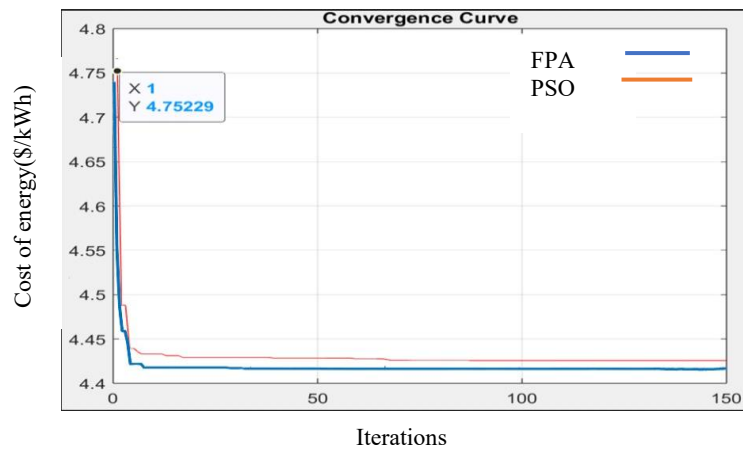

Fig. 6 The output power from the PV.

Fig. 7 Comparison of convergence rate of FPA and PSO.

4. Conclusion

The design and optimization of Concentrated Solar Power-Photovoltaic (CSP-PV) hybrid systems are important topics in the field of solar energy. In this study, we present a method for the optimal sizing of an autonomous microgrid comprising CSP/PV/DG components, based on a recently introduced metaheuristic algorithm called Flower Pollination Optimization (FPO). The microgrid sizing aims to fully meet the energy demand of an AC residential load. The climatic conditions in Libya, where the analysis was conducted, are excellent for the deployment of CSP-PV plants.

Our findings indicate that the FPO method demonstrates the ability to attain a global optimum with relatively simple computational requirements and achieves fast computational convergence when compared to benchmarked algorithms. Nevertheless, the utilization of the proposed algorithm can address some of the technical challenges that hinder microgrid projects. Furthermore, it can serve as a valuable tool to support off-grid rural electrification projects.

ORCID

Ahmed Moh A Al Smin https://orcid.org/0009-0003-2716-4136

Alkbir Munir Faraj Almabrouk https://orcid.org/0000-0001-7652-8141

Sairul Izwan Bin Safie https://orcid.org/0000-0003-1079-5014

Mohd Al Fatihhi Bin Mohd Szali Januddi https://orcid.org/0000-0001-7652-8141

Mohd Fahmi Bin Hussin https://orcid.org/0000-0003-3810-7148

Abdulgader Alsharif https://orcid.org/0000-0003-3515-4168

Declaration of Conflict of Interest

The authors declared that there is no conflict of interest with any other party on the publication of the current work.

References

[1] J.A. Aguilar-Jiménez, N. Velázquez, A. Acuña, R. Cota, E. González, L. González, R. López, S. Islas, Techno-economic analysis of a hybrid PV-CSP system with thermal energy storage applied to isolated microgrids, Solar Energy 174 (2018) 55–65. https://doi.org/10.1016/j.solener.2018.08.078.

[2] A. Alsharif, C.W. Tan, R. Ayop, A. Al Smin, A. Ali Ahmed, F.H. Kuwil, M.M. Khaleel, Impact of electric Vehicle on residential power distribution considering energy management strategy and stochastic Monte Carlo algorithm, Energies 16 (2023) 1358. https://doi.org/10.3390/en16031358.

[3] A.A.A.B. Amira, L.E. Vafaei, Application of PV for electricity generation in tajoura heart hospital ICU-Libya & applied at near east hospital, in: 2020 4th International Symposium on Multidisciplinary Studies and Innovative Technologies (ISMSIT), IEEE, 2020. https://doi.org/10.1109/ISMSIT50672.2020.9254227.

[4] A.O.M. Maka, J.M. Alabid, Solar energy technology and its roles in sustainable development, Clean Energy 6 (2022) 476–483. https://doi.org/10.1093/ce/zkac023.

[5] I. Arias, J. Cardemil, E. Zarza, L. Valenzuela, R. Escobar, Latest developments, assessments and research trends for next generation of concentrated solar power plants using liquid heat transfer fluids, Renewable and Sustainable Energy Reviews 168 (2022) 112844. https://doi.org/10.1016/j.rser.2022.112844.

[6] R. Zhai, Y. Chen, H. Liu, H. Wu, Y. Yang, Optimal design method of a hybrid CSP-PV plant based on genetic algorithm considering the operation strategy, International Journal of Photoenergy 2018 (2018) 1–15. https://doi.org/10.1155/2018/8380276.

[7] H. Liu, R. Zhai, J. Fu, Y. Wang, Y. Yang, Optimization study of thermal-storage PV-CSP integrated system based on GA-PSO algorithm, Solar Energy 184 (2019) 391–409. https://doi.org/10.1016/j.solener.2019.04.017.

[8] Y. Kherbiche, N. Ihaddadene, R. Ihaddadene, F. Hadji, J. Mohamed, A.H. Beghidja, Solar energy potential evaluation. Case of study: M'Sila, an Algerian province, International Journal of Sustainable Development and Planning 16 (2021) 1501–1508. https://doi.org/10.18280/ijsdp.160811.

[9] G. Photovoltaic, P. Potential, and C. F. Page, Libya, no. 2018, pp. 1–3, 2021.

[10] A.L. Bukar, C.W. Tan, K.Y. Lau, Optimal sizing of an autonomous photovoltaic/wind/battery/diesel generator microgrid using grasshopper optimization algorithm, Solar Energy 188 (2019) 685–696. https://doi.org/10.1016/j.solener.2019.06.050.

[11] A. Alsharif, C.W. Tan, R. Ayop, K.Y. Lau, A.M. Dobi, A rule-based power management strategy for Vehicle-to-Grid system using antlion sizing optimization, Journal of Energy Storage 41 (2021) 102913. https://doi.org/10.1016/j.est.2021.102913.

[12] R. Zhai, H. Liu, Y. Chen, H. Wu, Y. Yang, The daily and annual technical-economic analysis of the thermal storage PV-CSP system in two dispatch strategies, Energy Conversion and Management 154 (2017) 56–67. https://doi.org/10.1016/j.enconman.2017.10.040.

[13] X. Wang, Y. Wang, K. Chen, X. Bin, Z. Zhou, H. Peng, Global optimization of CSP-PV Hybrid System using an Artificial Fish-Swarm Algorithm, in: 2019 Chinese Automation Congress (CAC), IEEE, 2019. https://doi.org/10.1109/CAC48633.2019.8996573.

[14] Y. Zhang and S. J. Smith, Long-term modeling of solar energy: analysis of concentrating solar power (CSP) and PV technologies, 2008.

[15] W. P. S. in Energy, The Performance of Concentrated Solar Power (CSP) Systems, Peter Hell. Woodhead Publishing Series in Energy, 2017.

[16] S. Pramanik, R.V. Ravikrishna, A review of concentrated solar power hybrid technologies, Applied Thermal Engineering 127 (2017) 602–637. https://doi.org/10.1016/j.applthermaleng.2017.08.038.

[17] B. Belgasim, Y. Aldali, M.J.R. Abdunnabi, G. Hashem, K. Hossin, The potential of concentrating solar power (CSP) for electricity generation in Libya, Renewable and Sustainable Energy Reviews 90 (2018) 1–15. https://doi.org/10.1016/j.rser.2018.03.045.